IDR NEUTRINO FACTORY FRONT END AND VARIATIONS*

D. Neuffer, Fermilab, Batavia IL 60510, USA
A. Alekou, Imperial College, London UK; C. Rogers, Rutherford Appleton Laboratory, UK
P. Snopok, IIT, Chicago, IL 60166 USA; C. Yoshikawa, Muons, Inc., Batavia IL 60510 USA

Abstract

The (International Design Report) IDR neutrino factory scenario for capture, bunching, phase-energy rotation and initial cooling of μ's produced from a proton source target is explored. It requires a drift section from the target, a bunching section and a ϕ-δE rotation section leading into the cooling channel. Optimization and variations are discussed. Important concerns are rf limitations within the focusing magnetic fields and large losses in the transport.

INTRODUCTION

In a neutrino factory, short, intense bunches of protons are focused onto a target to produce pions, which decay into muons and are then accelerated into a high-energy storage ring, where their decays provide beams of high-energy neutrinos.[1, 2, 3] The challenge is to collect and accelerate as many muons as possible. The IDR neutrino factory consists of:

- a proton source with an intensity of 4 MW beam power (50 Hz, 8 GeV protons, ~2 ns bunches),
- a Front End system that produces π's that decay into μ's and forms them into cooled bunches,
- an accelerator that takes the μ's to ~25 GeV for insertion into storage rings. μ decays in the ring straight sections provide high-energy ν beams for:
- ~100 kton ν-detectors placed at 4000-7500km baselines.

The goal is > 10^{21} ν's/beamline/year in order to obtain precise measurements of ν-oscillation parameters.

FRONT END OVERVIEW

This paper describes the Front End system, which consists of the capture and cooling section that takes the π's produced at the target, and captures and cools the resulting decay μ's, preparing them for the μ accelerators. Fig. 1 shows an overview of the system.

Target and Decay Channel

The 5-15 GeV proton source produces short pulses of protons that are focused onto a liquid-Hg-jet target immersed in a high-field solenoid with an internal beam pipe radius r_{sol}. The proton bunch length is 1 to 3 ns rms (~5 to 15 ns full-width), B_{sol} =20 T, and r_{sol} = 0.075 m. Secondary particles are radially captured if they have a transverse momentum p_T less than ~$ecB_{sol}r_{sol}/2$ = 0.225 GeV/c. Downstream of the target solenoid the magnetic field is adiabatically reduced from 20T to 1.5T over ~15 m, while the beam pipe radius increases to 0.25 m. This arrangement captures a secondary pion beam with a broad energy spread (~50 MeV to 400 MeV kinetic energy).

The initial proton bunch is relatively short, and as the secondary pions drift from the target they spread apart longitudinally, following: $c\tau(s) = s/\beta_z + c\tau_0$, where s is distance along the transport and $\beta_z = v_z/c$. Hence, downstream of the target, the pions and their daughter muons develop a position-energy correlation in the RF-free drift. In the IDR baseline, the drift length is L_D = 64.6 m, and at the end of the decay channel there are about 0.2 muons of each sign per incident 8 GeV proton.

RF Buncher

The drift channel is followed by a buncher section that uses rf cavities to form the muon beam into a train of bunches, and a phase-energy rotating section that decelerates the leading high-energy bunches and accelerates the later low-energy bunches to the same mean energy.[4] To determine the buncher parameters, we consider reference particles (0, *N*) at P_0= 233 MeV/c and P_N = 154 MeV/c, with the intent of capturing muons from a large initial energy range (~50 to ~400 MeV). The rf frequency f_{rf} and phase are set to place these particles at the center of bunches while the rf voltage increases along the transport. This requires that the rf wavelength λ_{rf} increases, following:

$$N_B\lambda_{rf}(s) = N_B\frac{c}{f_{rf}(s)} = s\left(\frac{1}{\beta_N}-\frac{1}{\beta_0}\right)$$

where *s* is the total distance from the target, β_1 and β_2 are the velocities of the reference particles, and *N* is an integer. For the IDS, *N* is chosen to be 10, and the buncher length is 33m. Therefore, the rf cavities decrease in frequency from ~320 MHz (λ_{rf}= 0.94 m) to ~230 MHz (λ_{rf}= 1. 3m) over the buncher length.

The initial geometry for rf cavity placement uses 0.5 m long cavities placed within 0.75 m long cells. The 1.5T solenoid field focusing of the decay region is continued through the Buncher and the Rotator. The rf gradient is increased along the buncher, and the beam is captured into a string of bunches, each of them centered about a test particle position with energies determined by the $\delta(1/\beta)$ spacing from the initial test particle:

$$1/\beta_n = 1/\beta_0 + n\,\delta(1/\beta),$$

where $\delta(1/\beta)=(1/\beta_N - 1/\beta_0)/N$. In the initial design, the cavity gradients follow a linear increase along the buncher: $V'_{rf}(z) \approx 9(z/L_{Bf})\,MV/m$ where *z* is distance along the buncher. The gradual increase of voltage enables a somewhat adiabatic capture of muons into separated bunches.

*Work supported by DOE under contract DE-AC02-07CH11359.
#neuffer@fnal.gov

Copyright © 2012 by IEEE – cc Creative Commons Attribution 3.0 (CC BY 3.0) — cc Creative Commons Attribution 3.0 (CC BY 3.0)

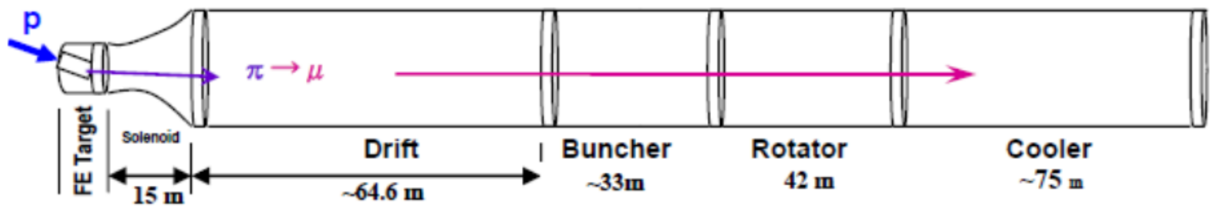

Figure 1: Overview of the IDR neutrino factory front end, consisting of a target solenoid (20 T), a capture solenoid (20 T to 1.5T, 15 m), Drift section (64.6 m), rf Buncher (33 m), an energy-phase Rotator (42 m), and a Cooler (75 m).

Table 1: Summary of Front end RF Requirements

Region	Length (m.)	Number of Cavities	Number of frequencies	Frequencies [MHz]	Peak Gradient {MV/m]	Peak Power requirements
Buncher	33	37	13	319.6 to 233.6	4 to 7.5	1 to 3.5 MW/freq.
Rotator	42	56	15	230.2 to 202.3	12	2.5 MW/cavity
Cooler	75	100	1	201.25	15	4 MW/cavity
Total (with Drift)	230m	193	29	319.6 to 201.25	1000 MV	550 MW

In practical implementation this linear ramp of varying-frequency cavities is approximated by a sequence of rf cavities that decrease in frequency along the 33 m length of the buncher. A total of 37 rf cavities are specified, with frequencies varying from 319.6 to 233.6, and rf gradients from 4 to 7.5 MV/m The number of different rf frequencies is limited to a more manageable 13 (~3 rf cavities per frequency). Table 1 lists the rf cavity requirements. At the end of the buncher, the beam is formed into a train of positive and negative bunches of different energies.

Phase-Energy Rotator

In the rotator section, the rf bunch spacing between the reference particles is shifted away from the integer N_B by an increment δN_B, and phased so that the high-energy reference particle is stationary and the low-energy one is uniformly accelerated to arrive at the high-energy at the end of the Rotator. For the IDS, $\delta N_B = 0.05$ and the bunch spacing between the reference particles is $N_B + \delta N_B = 10.05$. The Rotator consists of 0.75 m long cells with 0.5 m RF cavities at 12 MV/m. The frequency of cavities decreases from 230.2 MHz to 202.3 MHz down the length of the 42 m long rotator region. The rotator uses 54 RF cavites of 15 different frequencies. (see Table 1) At the end of the rotator the RF frequency matches into the ionization cooling channel (201.25 MHz).

Cooling Channel

The IDR baseline cooling channel design consists of a sequence of identical 1.5 m long cells (Fig. 2). Each cell contains two 0.5 m-long cavities, with 1.1cm thick LiH blocks at the ends of each cavity (4 per cell) and a 0.25 m spacing between cavities with solenoidal focusing coils. The LiH provides the energy loss material for ionization cooling. The total length of the cooling section is ~75m (50 cells). Based on simulations, the cooling channel reduces the transverse emittance by a factor of 2.5.

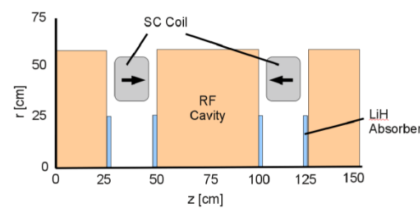

Figure 2: A cooling cell (schematic view).

In the IDR, the design concept is being developed into engineering detail in order to generate accurate cost estimates. In that process the component dimensions are shifted to meet construction constraints. For example, the cooling multi-cell design is shown in Fig. 3. Acceptance should be approximately unchanged.

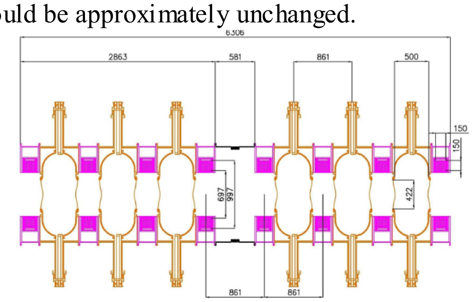

Figure 3: Cooling cells (engineering view).

STUDIES AND VARIATIONS

The μ accelerator has a restricted aperture that is approximated by accepting μ's with transverse amplitudes < 0.03 m and longitudinal amplitudes < 0.15 m (as defined in ref. 5). In simulations this accepted beam has a rms transverse emittance of $\varepsilon_{N,rms} \cong 0.004$ m, and the longitudinal emittance is ~0.036 m/bunch. At the end of the cooling channel there are interlaced trains of bunches of μ^+ and μ^-, of similar intensity. The trains are ~80m long (~54 bunches). Each bunch has an rms length of 0.15m, and an rms momentum width of ~30 MeV/c, with a mean momentum of ~250 MeV/c. ~0.1 μ+ and μ^- per

Copyright © 2012 by IEEE – cc Creative Commons Attribution 3.0 (CC BY 3.0) — cc Creative Commons Attribution 3.0 (CC BY 3.0)

ISBN 978-3-95450-115-1

initial 8 GeV proton are within acceptances. This has been simulated using the 3-D codes.[6, 7]

Beam Losses and Chicane/Absorber

In the front end, ~4 MW of proton beam is placed on target, producing ~25 kW of ~200 MeV μ's that are captured, along with a large number of uncaptured secondaries. These deposit a large amount of particle energy throughout the Front End system. Beam losses must be separated from superconducting magnet coils, and uncontrolled losses must be limited. Without any shielding or collimation for loss control, losses are at the ~100 W/m scale.

A chicane and absorber immediately following the capture solenoid can localize most losses to this initial portion of the system. The chicane is designed to transmit low-momentum particles; particles with p > ~500MeV/c hit the walls and do not follow downstream. The chicane bends out by 12.5° over 5 m and back by the same angle over 5 more m. (This displaces the beam channel by ~1.1m, see fig. 4) It removes high-energy protons, which would be lost throughout the transport, and also high-energy muons which would be out of time and phase with the captured beam. The same chicane filters both positive and negatives.

The chicane would be followed by an absorber (~10cm Be) that removes low-energy particles, particularly protons. The absorber and chicane distort the beam energy/phase relationship and the frequency/position of RF cavities in the buncher/rotator must be rematched. After rematching, the loss of accepted μ is ~10%, but the background of uncaptured beam is greatly reduced. An optimum design for the system and an assessment of the remnant losses is needed before incorporation of the concept into the final design.

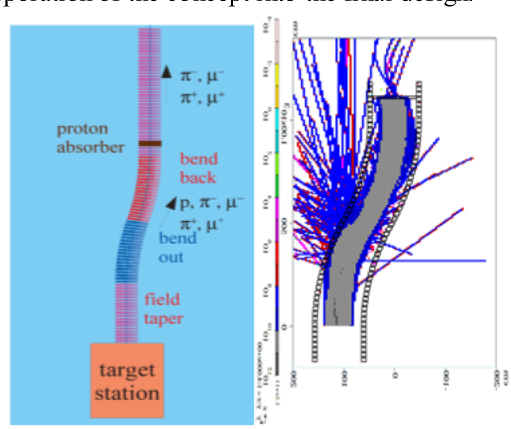

Figure 4: Chicane design concept, and particle loss trajectories from simulation.

RF Gradients in Magnetic Fields

The present configuration requires relatively high gradient RF cavities within strong solenoidal fields (~12 MV/m at ~200 MHz within ~1.5 T in the Rotator, and ~15 MV/m within alternating solenoids in the Cooler). Experimental studies show that RF cavities within magnetic fields may break down at smaller gradients.

The Front End design can be adapted to RF gradient limitations. A simplest adaptation is to maintain the design but use reduced gradients. Studies of reduced gradient operation indicate that reduction by as much as a factor of 2 would only reduce μ acceptance by ~30%.

Alternative designs that directly reduce the magnetic field and rf effects have also been developed. These include designs with gas-filled RF cavities, magnetically insulated RF systems, magnetically shielded cavities, and bucked coil configurations.

A particularly compelling alternative is the bucked coil geometry.[8] In the baseline channel, coils are close to the rf cavities, increasing peak fields on cavity surfaces to >4T. The opposing currents in the bucked coils reduce these off-axis fields to <2T (~1T in one example), while maintaining on-axis fields near the baseline values to obtain similar cooling.

REFERENCES

[1] M. Appollonio et al., "Accelerator Concept for Future Neutrino Facilities", RAL-TR-2007-23, *JINST* **4** P07001 (2009).

[2] "Cost-effective Design for a Neutrino Factory", J. S. Berg *et al.*, Phys**.** Rev. STAB **9**, 011001(2006).

[3] C. Ankenbrandt et al., "Low-Energy Neutrino Factory Design", Phys. Rev. STAB **12**, 070101(2009).

[4] D. Neuffer and A. Van Ginneken, Proc. PAC 2001, Chicago IL p.2029 (2001).

[5] R. Fernow, "Physics Analysis performed by ECALC9", MuCOOL-280, September 2003.

[6] R. Fernow et al. "ICOOL", Proc. 1999 PAC, NY, p. 3020, see http://pubweb.bnl.gov/people/fernow/

[7] T. J. Roberts et al., G4BeamLine 2.06 (2010), http://g4beamline.muonsinc.com

[8] A. Alekou et al. , this proceedings (2012).

Copyright © 2012 by IEEE – cc Creative Commons Attribution 3.0 (CC BY 3.0) — cc Creative Commons Attribution 3.0 (CC BY 3.0)